



Cite this: *Analyst*, 2025, **150**, 5374

Received 10th February 2025,  
Accepted 26th August 2025

DOI: 10.1039/d5an00152h

rsc.li/analyst

## Differentiation of cisplatin uptake within a population of cancer cells – how to “crack this nut” using single-cell ICP-MS

Zuzanna Szymańska,<sup>a</sup> Magdalena Matczuk,<sup>a</sup> Agnieszka Żuchowska,<sup>b</sup>  
Paweł Romańczuk,<sup>b</sup> Andrei R. Timerbaev<sup>c</sup> and Maciej Jarosz<sup>a</sup>

**A versatile tool to unravel the uptake diversity of a front-line anti-cancer drug, cisplatin, within a cancer cell population is proposed herein based on single-cell inductively coupled plasma mass spectrometry. The interested researcher is provided with a tutorial to help adapt such cutting-edge methodology and know-how to reliable data processing.**

Cisplatin is one of the platinum(II)-based drugs widely used to treat many tumors. Despite some limitations, such as side effects and intrinsic or acquired resistance,<sup>1,2</sup> cisplatin shows exceptional effectiveness in curing cancer alone or in combinatorial chemotherapy. As for other anticancer drugs, cellular uptake governs their treatment efficacy, and a low level of cisplatin in cancer cells reduces tumor response.<sup>1</sup> Furthermore, differences between cells even belonging to the same population significantly impact the response to cisplatin treatment.<sup>3</sup> This is because they may differ in size, physiological state, access to drugs, etc.<sup>4</sup>

Conventional inductively coupled plasma mass spectrometry (ICP-MS) holds a top position in *in vitro* uptake measurements of metal-based drugs.<sup>5,6</sup> Traditional cellular assays are conducted using the entire population of cells, which are digested, and the total amount of a metallodrug in a bulk sample is quantified. This strategy affords a general overview of fundamental intracellular mechanisms and processes.<sup>7,8</sup> However, the results can shed light only on an average response to drug treatment, assuming – correctly or not – that it is the same for every cell in the population. In fact, certain specific characteristics of individual cells may be concealed when using such a measurement strategy.<sup>7,9–11</sup> Considering the heterogeneity of cells, traditional ICP-MS ana-

lysis is deficient in obtaining sufficient information on drug internalization within the entire cell population and guiding the effectiveness of treatment.<sup>12</sup>

A promising modification of ICP-MS to respond to this challenge is single-cell ICP-MS (SC-ICP-MS).<sup>13–15</sup> This technique allows for quantifying elements in each cell from a given population, with their integrity preserved until they are individually transported into the plasma. A sufficiently short dwell time is mandatory to monitor signals from individual cells. In such an operational mode, the number of peaks corresponds to the number of cells, while the peak intensity is related to the content of a target element in the cell. The use of SC-ICP-MS also requires a suitable sample introduction system, as with conventional nebulizers, transport efficiency is usually less than 1%.<sup>9,14,17</sup> The special nebulizers and spray chambers with an additional make-up gas stream designed for SC analysis can significantly increase transport efficiency.<sup>13,16</sup> Also, the cell suspension should be diluted appropriately (to about  $1 \times 10^5$  cells per mL).<sup>4</sup>

The application of SC-ICP-MS for measuring cisplatin uptake and other Pt-based drugs in various cell lines has already been attempted,<sup>18–23</sup> with cisplatin quantified in single cells and isolated nuclei.<sup>23</sup> Also, the uptake of other metallodrugs has been explored using SC-ICP-MS.<sup>24–26</sup> However, these studies are not free of shortcomings. First of all, the sample preparation is often a multi-step and time-consuming process. When the sample is diluted before analysis (to a certain cell concentration), it is done in variable proportions for each sample. Moreover, a cell fixation process is typically required to preserve samples until analysis.<sup>19,21,24,25</sup> Another missing issue is the actual dose of the drug, usually unspecified in terms of the volume of a metallodrug solution. Last but not least, data treatment varies from one study to another. More specifically, the threshold values for cell detection are set manually, which is subjective,<sup>19</sup> or fixed the same for all types of samples.<sup>21,25</sup> It should be pointed out in this context that although several brands of data treatment software are

<sup>a</sup>Chair of Analytical Chemistry, Warsaw University of Technology, Noakowskiego St. 3, 00-664 Warsaw, Poland. E-mail: magdalena.matczuk@pw.edu.pl

<sup>b</sup>Chair of Medical Biotechnology, Warsaw University of Technology, Noakowskiego St. 3, 00-664 Warsaw, Poland

<sup>c</sup>Institute of Inorganic Chemistry, University of Vienna, Währinger Str. 42, 1090 Vienna, Austria



available, they are primarily designed for single-particle analysis.<sup>27</sup>

To this end, our first-principles investigation has been inspired by the need to unveil cisplatin uptake at the individual cell level using a purpose-upgraded SC-ICP-MS technique. With this objective, special attention was paid to the experimental factors affecting the reliability of SC measurements, regardless of the metallodrug or cell nature. Another critical issue was developing an effective data treatment protocol to analyze the SC results appropriately. As proof of principle, the impact of drug-loading parameters, *viz.*, the dose and incubation time, on the variability of cisplatin uptake within the cell population was tested to verify the accuracy of the developed methodology.

The cells (MDA-MB-231 line; *ca.*  $5 \times 10^5$  in each sample) were incubated with cisplatin (0.5, 1, or 5 ppm) for 5 or 24 h (see the SI for more details), washed thoroughly with PBS, collected using TrypLE™ Express (Gibco, Thermo Fisher Scientific, Waltham, USA), and resuspended in 1 mL of fresh culture medium (Fig. 1). MDA-MB-231 cells were chosen due to their resistance to cisplatin treatment and hence preserved integrity until analysis.

All experiments were performed using an Agilent 8900 ICP QQQ mass spectrometer (Agilent Technologies, Santa Clara, USA) and a microFAST SC automated sample introduction system (Elemental Scientific, Omaha, USA) with a CytoNeb nebulizer and a CytoSpray spray chamber. The operational conditions shown in Table S1 were found apt to detect SC events, ensure adequate cell transportation into the plasma without damaging the structure, and obtain the highest sensitivity of the platinum signal. Cell counting was carried out using a plate reader, Cytation3 (BioTek, Winooski, USA).

Initially, we attempted to visualize the results using MassHunter Workstation Software in Single Particle Mode (Agilent Technologies). However, this software was inappropriate for SC calculations because of a bias in the cell detection threshold. Therefore, all data treatments were performed using an in-house developed script in MATLAB software, separating SC signals from the background and counting them. Fig. 2 shows the cell signals derived from the script. It should be emphasized that the most crucial part of data analysis was determining the cell detection threshold. For this purpose, an iterative procedure was applied. First, the mean value ( $\mu$ ) and the standard deviation ( $\sigma$ ) for the entire data set were calculated. Then, the data points above a  $\mu + 3\sigma$  threshold were col-

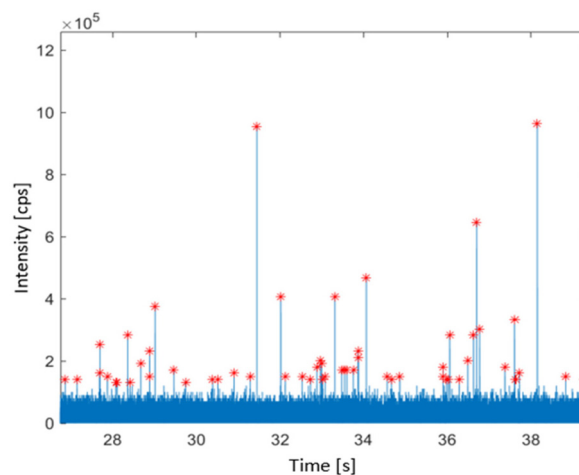


Fig. 2 An exemplary data treatment using the developed script in MATLAB software. Red points represent cell signals (after incubation with 1 ppm cisplatin for 24 h).

lected, and from the remaining points, the  $\mu$  and the  $\sigma$  were recalculated. This procedure was repeated until there were no more points to collect. A  $\mu + 3\sigma$  value from the last iterative step was the baseline level, while the points  $3\sigma$  above the baseline were treated as cell signals. Outliers were discarded empirically. The described script was highly effective for the quick and non-subjective calculation of the baseline signal (BS) value, cell detection threshold, and cell number determination in each sample. Combined with Microsoft Excel, it also enabled the estimation of the platinum amount in each cell.

The amount of platinum in single cells was determined as  $m_c = \eta FtI/a$ , where  $m_c$  is the mass of the element in each cell,  $\eta$  is the transport efficiency of calibration solutions,  $F$  is the sample flow rate,  $t$  is the dwell time,  $I$  is the signal intensity of the analyte in cells minus the signal intensity of background, and  $a$  is the slope of the calibration curve (see the SI for details).

Worth mentioning is the accuracy of the flow-rate ratio of nebulizer and make-up gases, essential for adequately transporting cells into the plasma without damaging their structure. (This issue is usually neglected in the above-cited SC-ICP-MS reports.) Our data (not shown) showed that this parameter significantly affects both the cell detection threshold and the number of detected cells. Not surprisingly, our studies also confirmed that the application of specified automated introduction systems capable of minimizing the flow of the sample (here,  $10 \mu\text{L min}^{-1}$  with microFAST *vs.*  $22 \mu\text{L min}^{-1}$  with a peristaltic pump) significantly reduces the BS intensity (Table 1), making the data analysis more convenient and the obtained results reliable.

Along with the nebulizer gas, make-up gas, and sample flow rates, the next element of optimization trials was examining the effect of sample dilution on BS and the number of detected cells. There was a noticeable variability in the BS between the samples of cells incubated with different concen-

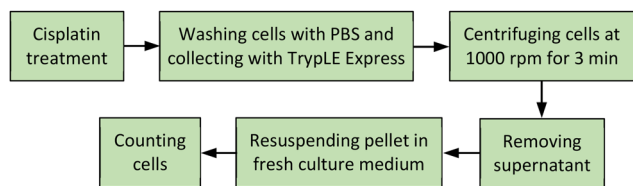


Fig. 1 A schematic diagram showing the workflow for sample preparation.



**Table 1** Effect of the sample flow rate on the baseline signal (BS)

Cisplatin [ppm]	10 $\mu\text{L min}^{-1}$		22 $\mu\text{L min}^{-1}$	
	BS [cps, $\times 10^3$ ]	$\sigma [\times 10^3]$	BS [cps, $\times 10^3$ ]	$\sigma [\times 10^3]$
0.5	41.2	5.4	46.7	8.2
1.0	62.8	19.7	75.4	2.2
5.0	189.3	26.7	225.4	29.2

trations of cisplatin. Therefore, the samples were diluted at various ratios. The best results were obtained when samples treated with 0.5 ppm cisplatin were not diluted, those fortified with 1 ppm cisplatin were diluted two-fold, and 5 ppm cisplatin samples were diluted five times. The appropriate dilution resulted in a decreased BS and an increased number of detected cells. As mentioned above, the samples were typically diluted to a certain concentration of cells, whereas in our approach, the number of cells was constant, regardless of the drug concentration.

Markedly, the cells were analyzed directly in the culture medium for the first time, streamlining the sample preparation procedure. In this context, it is essential to comprehend that cell-culture media are highly complex in composition and similarly intricate in discerning cell events from the BS. Notably, Pt is an element that does not exist in the cell medium under investigation, and this feature makes our SC-ICP-MS measurements feasible. We disregarded the option of cell fixation prior to analysis, as there is a possibility of analyte leaching from cells into the fixative agent.<sup>28</sup>

Next, the optimized SC-ICP-MS protocol was probed to prove the varying cisplatin uptake in the cell population due to differences in their size, age, cell-cycle status, tissue microenvironmental changes, or access to nutrients and drugs.<sup>3,4,12</sup> Not surprisingly, the amount of Pt in SCs depends on the drug concentration and incubation time, thus confirming the correctness of the adopted analytical procedure. It is worthwhile to mention that increasing the cisplatin concentration increases the BS, and hence, the cell detection threshold becomes higher. Other researchers who applied comparable cisplatin concentrations and incubation times have reported similar general relationships.<sup>18,19,21,22</sup> However, since different cell lines were explored, the results differ in the overall amounts of taken-up Pt. Whereas the reported median ranged from approximately 0.4 to 10 fg per cell,<sup>18,19,21,22</sup> our data on platinum accumulation were much lower, with a median of about 60 ag per cell (5 ppm cisplatin). The possible explanation for our substantially lower cellular levels may be the cisplatin resistance of MDA-MB-231 cells. The obtained results are summarized in Fig. 3–5.

Evidently, with a 5 h incubation time, the dispersion of the internalized Pt is much greater at 5 ppm cisplatin concentration than at lower concentrations (see Fig. 3). The data acquired at the incubation time of 24 h show lower between-concentration discrepancy; furthermore, the interquartile ranges for the 0.5 and 1 ppm samples are similar. For all box-

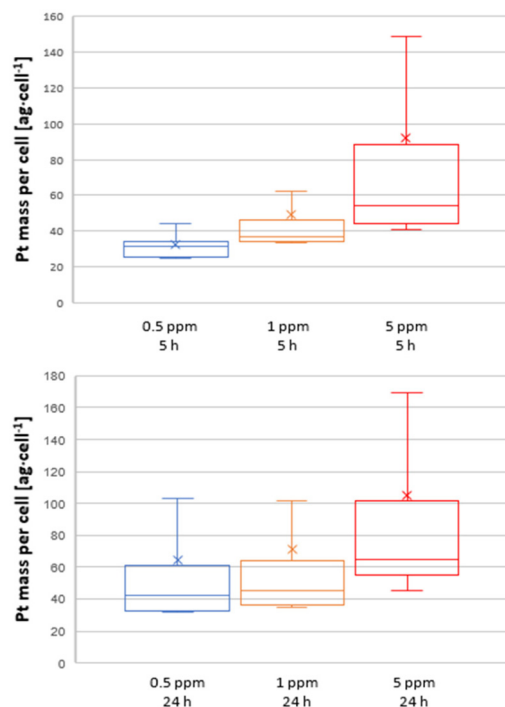


**Fig. 3** Cisplatin uptake measured with SC-ICP-MS. The interquartile ranges are represented by the height of the boxes. Lines inside the boxes denote the medians. Crosses indicate the means. The whisker represents the 1.5 interquartile range (minimum or maximum values without considering outliers).

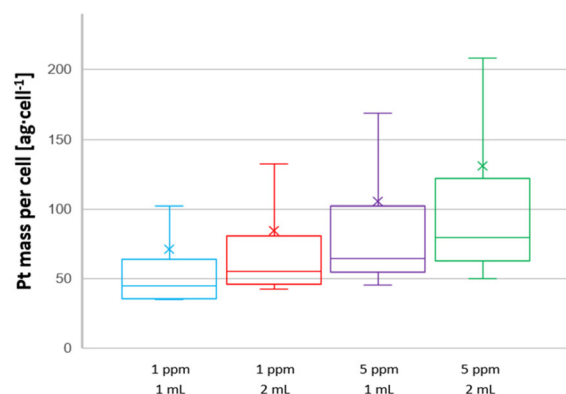


**Fig. 4** The Pt mass in cancer cells treated with varying concentrations and volumes of cisplatin solutions for 24 h. The interquartile ranges are represented by the height of the boxes. Lines inside the boxes denote the medians. Crosses indicate the means. The whisker represents the 1.5 interquartile range (minimum or maximum values without considering outliers).

plots, the median is smaller than the mean, which implies log-normal distributions (in more than 50% of cases, the Pt mass per cell has a value smaller than the mean). The medians and interquartile ranges for all concentrations are greater after 24 h of incubation. However, the amount of Pt in the cells does not increase linearly, which seems to be related to the



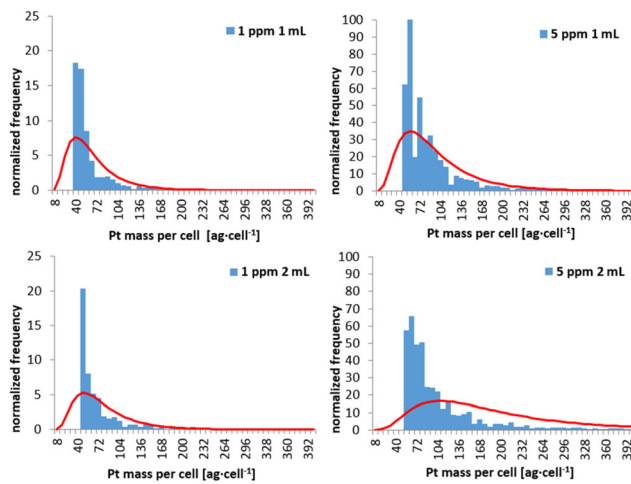


**Fig. 5** Histograms for the Pt mass in cancer cells treated for 24 h. The red lines represent the lognormal fit of the frequency.

mechanism of cisplatin internalization. The drug uptake rate is relatively high at the beginning of incubation, then decreases and levels off.<sup>29,30</sup> In our experiments, longer incubation times revealed more differences between cells, as indicated by wider interquartile ranges at 0.5 and 1 ppm concentrations.

Another (but predictable) observation is that the dispersion of platinum taken up in the cell population under scrutiny is the widest for the treatment with the highest drug dose. As can be seen in Fig. 4, the actual dose (or the number of moles of cisplatin in each sample) affects the drug uptake and BS. The number of moles is higher in the greater volume of the cisplatin solution at its specific concentration. Therefore, the volume of the drug solution should not be omitted from the report. Fig. 5 shows normalized histograms, illustrating the spread of cellular Pt contents.

Performing SC-ICP-MS measurements directly from the culture medium simplifies the analysis workflow. However, this approach should be further verified to be widely accepted by the bioanalytical community. This sample matrix comprises many components (proteins, organic acids, inorganic salts, *etc.*) that can pose spectral interferences or plasma suppression (as underlined by one of the anonymous reviewers). This issue can be at least in part circumvented by changing the medium or carrying out a blank analysis before real-world measurements. Importantly, direct SC-ICP-MS analysis is more consistent in the case of noble metal drugs, including Pt and Au compounds. Another important aspect is the BS dependence on the concentration of cisplatin (see above), where higher cisplatin doses could potentially increase the BS from the release of residually bound Pt on the surfaces of the cells. Therefore, in future work, we intend to prove whether the BS variabilities are unrelated to residual Pt in the medium by testing supernatants after washing the cells.

In conclusion, SC-ICP-MS holds promise as a tool for gaining insight into the heterogeneity of the cancer cell popu-

lation and the differentiation of cisplatin internalization. However, making SC-ICP-MS measurements accurate is a challenging task. Here, we have developed a novel strategy to portray the cisplatin uptake at a SC level and, notably, an original approach for data treatment. Notwithstanding, the authors did not overlook that in real-world circumstances, cisplatin enters the cell not as an intact drug but after (numerous) extracellular transformations. Indeed, whichever the active form of cisplatin is, it will be similarly recorded due to the element-specific nature of ICP-MS, and likewise for any other metal-based drug subjected to SC-ICP-MS analysis. As a final remark, detailed information about differences in drug affinity between cancer cells might serve as a basis for developing personalized oncomedicine.

## Conflicts of interest

There are no conflicts to declare.

## Data availability

Some of the data supporting this article have been included as part of the SI, and the rest will be available upon request.

Supplementary information is available. See DOI: <https://doi.org/10.1039/d5an00152h>.

## Acknowledgements

This research has been supported by the POSTDOC 1 PW (1820/128/Z01/Z10/2021) and Lab-Tech of Excellence 1 (1820/83/Z01/2022) projects, funded by the Warsaw University of Technology within the Excellence Initiative: Research University (IDUB) programme; Warsaw University of Technology.

## References

- 1 R. L. Lucaciu, A. C. Hangan, B. Sevastre and L. S. Oprean, *Molecules*, 2022, **27**, 6485.
- 2 S. Ghosh, *Bioorg. Chem.*, 2019, **88**, 102925.
- 3 L. Yang, J. George and J. Wang, *Proteomics*, 2020, **20**, 1900226.
- 4 B. Michalke, *Int. J. Mol. Sci.*, 2022, **23**, 6109.
- 5 A. R. Timerbaev, *J. Anal. At. Spectrom.*, 2014, **29**, 1058–1072.
- 6 A. R. Timerbaev, *J. Anal. At. Spectrom.*, 2021, **36**, 254–266.
- 7 M. Tajik, M. Baharfar and W. A. Donald, *Trends Biotechnol.*, 2022, **40**, 1374–1392.
- 8 S. Meyer, A. López-Serrano, H. Mitze, N. Jakubowski and T. Schwerdtle, *Metallomics*, 2018, **10**, 73–76.
- 9 C. Davidson, D. Beste, M. Bailey and M. Felipe-Sotelo, *Anal. Bioanal. Chem.*, 2023, **415**, 6931–6950.
- 10 P. Hu, W. Zhang, H. Xin and G. Deng, *Front. Cell Dev. Biol.*, 2016, **4**, 1–12.



- 11 A. Schmid, H. Kortmann, P. S. Dittrich and L. M. Blank, *Curr. Opin. Biotechnol.*, 2010, **21**, 12–20.
- 12 S. F. Nassar, K. Raddassi and T. Wu, *Metabolites*, 2021, **11**, 729.
- 13 M. Corte-Rodríguez, R. Álvarez-Fernández, P. García-Cancela, M. Montes-Bayón and J. Bettmer, *Trends Anal. Chem.*, 2020, **132**, 116042.
- 14 S. Theiner, K. Loehr, G. Koellensperger, L. Mueller and N. Jakubowski, *J. Anal. At. Spectrom.*, 2020, **35**, 1784–1813.
- 15 X. Yu, M. He, B. Chen and B. Hu, *Anal. Chim. Acta*, 2020, **1137**, 191–207.
- 16 L. Rasmussen, H. Shi, W. Liu and K. B. Shannon, *Anal. Bioanal. Chem.*, 2022, **414**, 3077–3086.
- 17 A. B. S. da Silva and M. A. Z. Arruda, *J. Trace Elem. Med. Biol.*, 2023, **75**, 127086.
- 18 M. Corte Rodríguez, R. Álvarez-Fernández Garcia, E. Blanco, J. Bettmer and M. Montes-Bayón, *Anal. Chem.*, 2017, **89**, 11491–11497.
- 19 S. Y. Lim, Z. E. Low, R. P. W. Tan, Z. C. Lim, W. H. Ang, T. Kubota, M. Yamanaka, S. Pang, E. Simsek and S. F. Y. Li, *Metallomics*, 2022, **14**(12), mfac085.
- 20 L. Gutiérrez-Romero, E. Blanco-Gonzalez and M. Montes-Bayón, *Anal. Chem.*, 2023, **95**, 11874–11878.
- 21 T. Liu, E. Bolea-Fernandez, C. Mangodt, O. De Wever and F. Vanhaecke, *Anal. Chim. Acta*, 2021, **1177**, 338797.
- 22 D. Turiel-Fernández, L. Gutiérrez-Romero, M. Corte-Rodríguez, J. Bettmer and M. Montes-Bayón, *Anal. Chim. Acta*, 2021, **1159**, 338356.
- 23 A. Galé, L. Hofmann, N. Lüdi, M. N. Hungerbühler, C. Kempf, J. T. Heverhagen, H. von Tengg-Kobligk, P. Broekmann and N. Ruprecht, *Int. J. Mol. Sci.*, 2021, **22**, 9468.
- 24 Z. Fan, J. Xie, R. Kushwaha, S. Liang, W. Li, A. A. Mandal, L. Wei, S. Banerjee and H. Huang, *Chem. – Asian J.*, 2023, **18**, e202300047.
- 25 D. Vicente-Zurdo, B. Gómez-Gómez, I. Romero-Sánchez, N. Rosales-Conrado, M. E. León-González and Y. Madrid, *Anal. Chim. Acta*, 2023, **1249**, 340949.
- 26 Z. Fan, Y. Rong, T. Sadhukhan, S. Liang, W. Li, Z. Yuan, Z. Zhu, S. Guo, S. Ji, J. Wang, R. Kushwaha, S. Banerjee, K. Raghavachari and H. Huang, *Angew. Chem., Int. Ed.*, 2022, **61**, e202202098.
- 27 M. I. Chronakis, B. Meermann and M. von der Au, *Anal. Bioanal. Chem.*, 2025, **417**, 7–13.
- 28 C. Davison, J. Pascoe, M. Bailey, D. J. V. Beste and M. Felipe-Sotelo, *Anal. Bioanal. Chem.*, 2024, **416**, 6945–6955.
- 29 V. Troger, J. L. Fischel, P. Formento, J. Gioanni and G. Milano, *Eur. J. Cancer*, 1992, **28**, 82–86.
- 30 A. W. El-Kareh and T. W. Secomb, *Neoplasia*, 2003, **5**, 161–169.

